

Article

Synthesis of GO-SalenMn and Asymmetric Catalytic Olefin Epoxidation

Fengqin Wang^{1,†}, Tiankui Huang^{1,†}, Shurong Rao^{1,†}, Qian Chen¹, Cheng Huang¹,
Zhiwen Tan², Xiyue Ding³ and Xiaochuan Zou^{1,*} 

¹ Department of Biological and Chemical Engineering, Chongqing University of Education, Nan'an 400067, China; wangfengqin0611@163.com (F.W.); xiaokui46485@163.com (T.H.); rao1334898571@163.com (S.R.); qian13340380042@163.com (Q.C.); HccVictory@163.com (C.H.)

² College of Chemistry, Chongqing Normal University, Chongqing 401331, China; tzw15310181725@163.com

³ College of Food and Biological Engineering, Jimei University, Xiamen 361021, China; xiyue772751020@163.com

* Correspondence: zouxc@cque.edu.cn; Tel.: +86-23-8630-7018; Fax: +86-23-6163-8000

† F.Q. Wang, T.K. Huang and S.R. Rao. contributed equally to this works.

Received: 9 September 2019; Accepted: 26 September 2019; Published: 30 September 2019



Abstract: Graphene oxide (GO) was used as a catalyst carrier, and after the hydroxyl group in GO was modified by 3-aminopropyltrimethoxysilane (MPTMS), axial coordination and immobilization with homogeneous chiral salenMnCl catalyst were carried out. The immobilized catalysts were characterized in detail by FT-IR, TG-DSC, XPS, EDS, SEM, X-ray, and AAS, and the successful preparation of GO-salenMn was confirmed. Subsequently, the catalytic performance of GO-salenMn for asymmetric epoxidation of α -methyl-styrene, styrene, and indene was examined, and it was observed that GO-salenMn could efficiently catalyze the epoxidation of olefins under an *m*-CPBA/NMO oxidation system. In addition, α -methyl-styrene was used as a substrate to investigate the recycling performance of GO-salenMn. After repeated use for three times, the catalytic activity and enantioselectivity did not significantly change, and the conversion was still greater than 99%. As the number of cycles increased, the enantioselectivity and chemoselectivity gradually decreased, but even after 10 cycles, the enantiomeric excess was 52%, which was higher than that of the homogeneous counterpart under the same conditions. However, compared to fresh catalysts, the yield decreased from 96.9 to 55.6%.

Keywords: graphene oxide; 3-aminopropyltrimethoxysilane; heterogeneous catalyst; asymmetric epoxidation

1. Introduction

Chiral salenMnCl catalyst (Jacobsen's catalyst) has been proved to be one of the most effective catalysts for asymmetric catalytic epoxidation of alkenes [1,2]. The chiral epoxides obtained are widely used in the synthesis of fine chemicals including pesticides, flavorings, and pharmaceuticals, such as the key intermediates for anti-hypertensive drugs and for the side chain of the anti-cancer drug paclitaxel. In most cases, homogeneous catalytic reactions are highly efficient. However, because it is difficult to separate and recycle the expensive chiral catalysts after the reaction, it is impossible to realize continuous flow reactors and large-scale production, which increases operating costs and wastes limited resources. Heterogeneity of homogeneous catalysts is an important strategy to enable the reuse of expensive chiral catalysts and large-scale synthesis [3]. Common catalytic carrier materials include organic polymer, inorganic solidseries, and organic polystyrene/inorganic hydrogen phosphate (Zr, Al, Zn, Ca) [4–15]. Unfortunately, immobilized catalysts still have some deficiencies such as low

catalytic efficiency and poor reusability. Therefore, developing a class of highly-efficient heterogeneous catalysts is still the focus of current studies.

In recent years, GO has been widely researched as a promising catalyst carrier [16], mainly because of its unique two-dimensional planar structure (which is beneficial to improve the dispersion of catalytic active species on the surface), higher specific surface area (which is beneficial to increase its forces with active species and, to a certain extent, prevent the migration and leaching of active species in the reaction process), and the nanometer size effect (which can improve the catalytic reaction rate). In addition, the surface of GO contains a large amount of oxygen-containing active groups, such as carboxyl, hydroxyl, and epoxy groups, which are easy to chemically modify [17] and can react with noble metal catalysts and homogeneous ligands to obtain various supported catalysts with different coordination modes. Hence, GO is widely used in organic catalysis [18,19], photocatalysis [20,21], and electrocatalysis [22]. Noble metal catalysts, such as Pd^{2+} , Pd^0 [18], and Au [19], can coordinate with GO to obtain composite catalysts that can be used for a cross-coupling reaction and an addition reaction between phenylacetylene and hydrogen, achieving efficient catalysis of the catalyst (up to 99%) with excellent catalyst stability. At the same time, GO successfully immobilizes Schiff-base ligands [23] and L-proline [24] homologous ligands through covalent grafting and clever use of hydrogen bonds and evaluates the catalytic activity of the Suzuki reaction in the water phase and the asymmetric catalytic aldol reaction, respectively. GO/Schiff-base catalysts can efficiently catalyze the Suzuki reaction of aryl halide in the water phase and aryl boric acid under mild conditions, and it was observed that the activity of the catalysts remained nearly unchanged after five repeated uses. GO/L-proline catalysts possess high catalytic activity and good reuse performance, and the asymmetric selectivity of catalytic reactions increases compared with homogeneous catalysts due to the unique layered structure of GO. It is considered that an obvious spatial confinement effect [25] appears in the nanosphere, which enhances the chiral inducibility of heterogeneous asymmetric reactions.

To continue to study the potential performance of GO as a catalyst carrier and further develop a simple heterogeneous epoxidation catalysts with good catalytic efficiency and high stability, we modified the hydroxyl groups in GO that were functionalized by MPTMS. Then, axial coordination fixation was carried out with the homogeneous chiral salenMnCl catalyst, to investigate in detail the catalytic performance of the supported catalyst for asymmetric epoxidation of α -methyl-styrene, styrene, and indene compared with the homogeneous catalyst. In addition, the catalytic oxidation of α -methyl-styrene was used as a template reaction to investigate the cyclic performance of the supported catalyst.

2. Results and Discussion

2.1. FT-IR Analysis

FT-IR spectroscopy results of GO, salenMnCl, and catalyst GO-salenMn are shown in Figure 1a–c. Figure 1a shows the FT-IR spectrum of GO. A very wide and strong absorption peak appeared between 3100 and 3500 cm^{-1} , which denoted the stretching vibration peak of hydroxyl groups (COO-H/O-H), indicating that GO contained hydroxyl and carboxyl groups. The absorption peak at approximately 1724 cm^{-1} indicated the stretching vibration peak of the carboxyl group (C=O). In addition, the absorption peaks at 1218 and 1050 cm^{-1} denoted the stretching vibration peaks of hydroxyl groups (C-OH) and the C-O bond of epoxy groups (C-O-C), respectively. The results showed that GO was successfully prepared by the Hummer method. Figure 1b shows the FT-IR spectrum of the homogeneous salenMnCl catalyst, showing that 2963–2864 cm^{-1} are the stretching vibration absorption peaks of methyl and methylene groups $\nu_{(\text{C-H})}$, respectively. Characteristic absorption peaks at 1610 cm^{-1} and 522 cm^{-1} were indicative of C=N and Mn-N bonds, respectively. In Figure 1c, 2936–2853 cm^{-1} were the stretching vibration absorption peaks of methyl and methylene groups $\nu_{(\text{C-H})}$, respectively. The absorption peak at approximately 1620 cm^{-1} in GO-salenMn denoted the stretching vibration of $\nu_{(\text{C}=\text{N})}$, which indicated that chiral heterogeneous catalysts possessed structures similar to those

of homogeneous chiral catalysts [26]. These results preliminarily confirmed the heterogeneity of homogeneous salenMnCl catalyst.

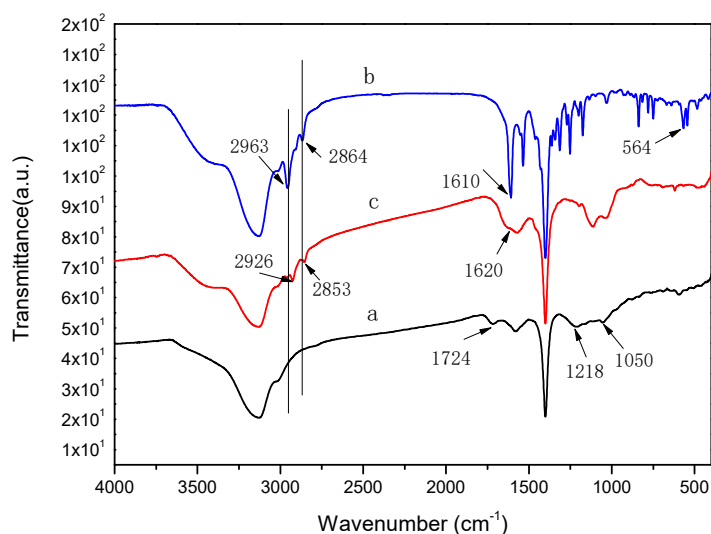


Figure 1. IR spectra of (a) GO, (b) salenMnCl, and (c) GO-salenMn.

2.2. TG–DSC Analysis

TG–DSC analysis of catalyst GO-salenMn is shown in Figure 2. Weightlessness was divided into three stages. The first stage was the heat absorption process at 120 °C room temperature. In this stage, the weight loss of water was approximately 15%, which was mainly due to the removal of water attached to the surface of the catalyst. The second stage was the strong exothermic process at 120 °C–500 °C. The weight loss of 32% during this stage was mainly due to the decomposition of oxygen-containing groups on graphene oxide and the decomposition of salenMn complexes. After 500 °C, weight loss slowed as the temperature increased. Finally, until 700 °C, the remaining mass of carbon skeleton and manganese oxide was approximately 38%.

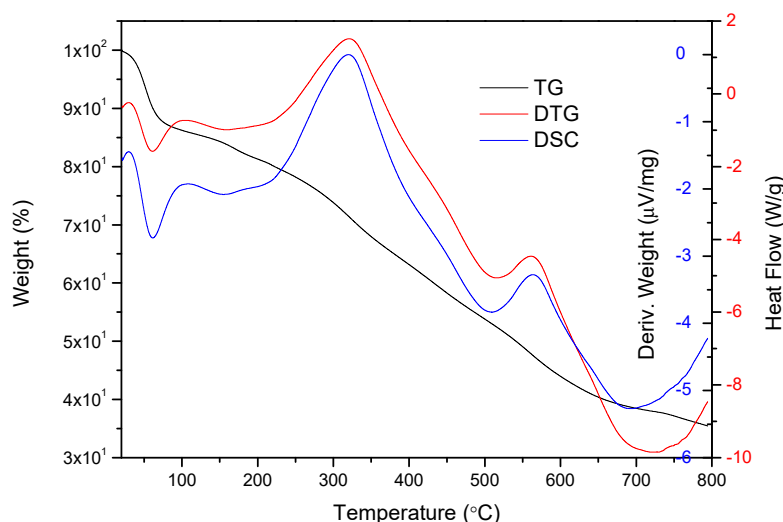


Figure 2. TG–DSC spectra of GO-salenMn.

2.3. XPS Analysis

XPS is an important method for analyzing metal valence on the surface of materials. The binding energy of the electrons in the center of the metal is affected by the differences in the electron environment, such as the oxidation state or the spin state. Figure 3 shows the full spectra of XPS scans of salenMn and

GO-salenMn. Figure 3a clearly shows the characteristic peaks of C1s, O1s, N1s, Mn 2p^{1/2}, and Mn 2p^{3/2} in homogeneous salenMn catalyst. In Figure 3b, in addition to the characteristic peaks in homogeneous salenMnCl, new-additional characteristic peaks, Si 2p and Si 2s, proved that GO successfully achieved the support of homogeneous salenMn after MPTMS modification. In addition, as seen in Figure 4, the electron binding energy of Mn2p^{3/2} in catalyst GO-salenMn was 641.4 eV, which was slightly higher than that of Mn2p^{3/2} in the homogeneous salenMnCl complex. Thus, the electron cloud density of manganese atoms decreased after support, which was similar with the reported value [8,27], possibly because the micro environment changed after metallic Mn was immobilized with 3-aminopropyl trimethoxy silane and modified GO. A similar observation has also been made for a chiral salenMn^{III} catalyst, which was axially grafted on an amine (–NH₂) group modified organic polymer/inorganic zirconium hydrogen phosphate through N–Mn bonding [28].

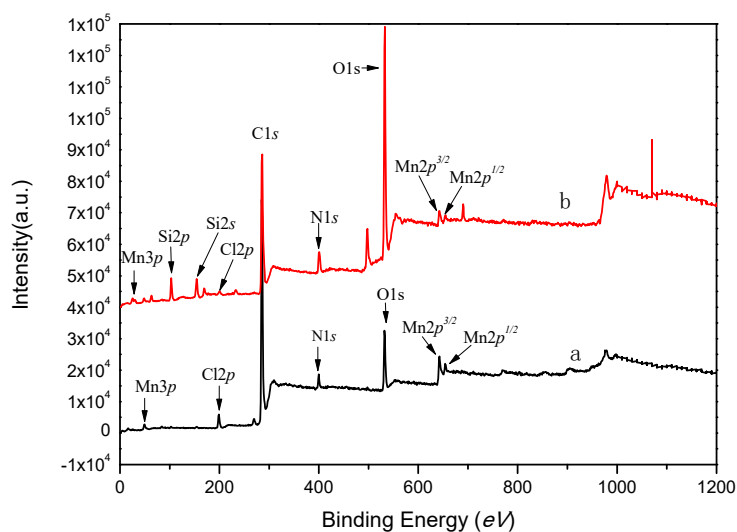


Figure 3. XPS spectra of (a) salenMn and (b) GO-salenMn.

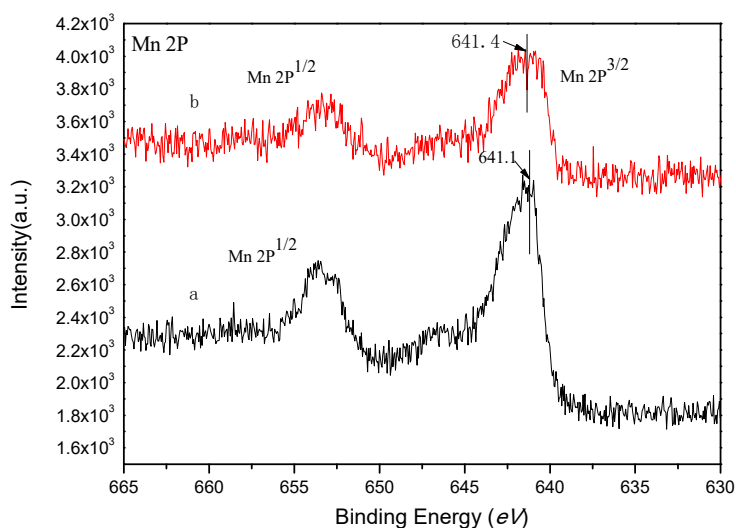


Figure 4. XPS spectra of Mn 2p for (a) salenMn and (b) GO-salenMn.

2.4. SEM and EDS Analysis

SEM images of GO, GO-NH₂, and GO-salenMn are shown in Figure 5a–c. As seen in Figure 5a, as a specific feature of GO, a large number of overlapping and curled slice layers existed, which indicated that GO had been successfully prepared. Figure 5b,c shows that the lamellar structure was damaged to a certain degree, which may have occurred after the amine and salenMn catalyst were introduced

on the surface of GO, and the inter-layer space subsequently increased. Under the influence of ultrasonic dispersion, slices of GO would strip, and the same conclusion could be drawn from XRD. To further confirm that chiral salenMnCl complexes were successfully immobilized on carrier GO, which was modified by MPTMS, EDS analysis of GO-salenMn was carried out (Figure 5d–f). The results showed that, compared with GO (Figure 5d), characteristic spectral lines of Si and N appeared in GO-NH₂ (Figure 5e), indicating that Si-containing amine functional groups were successfully introduced in GO. Compared with GO-NH₂ (Figure 5e), GO-salenMn (Figure 5f) exhibited obvious characteristic spectral lines of Mn, which also proved that MPTMS-modified GO successfully achieved axial immobilization with chiral salenMnCl complexes. In addition, according to Figure 6a–d, EDS layers of GO-salenMn contained elements such as C, O, Mn, and Si, which further proved the heterogeneity of chiral salenMnCl.

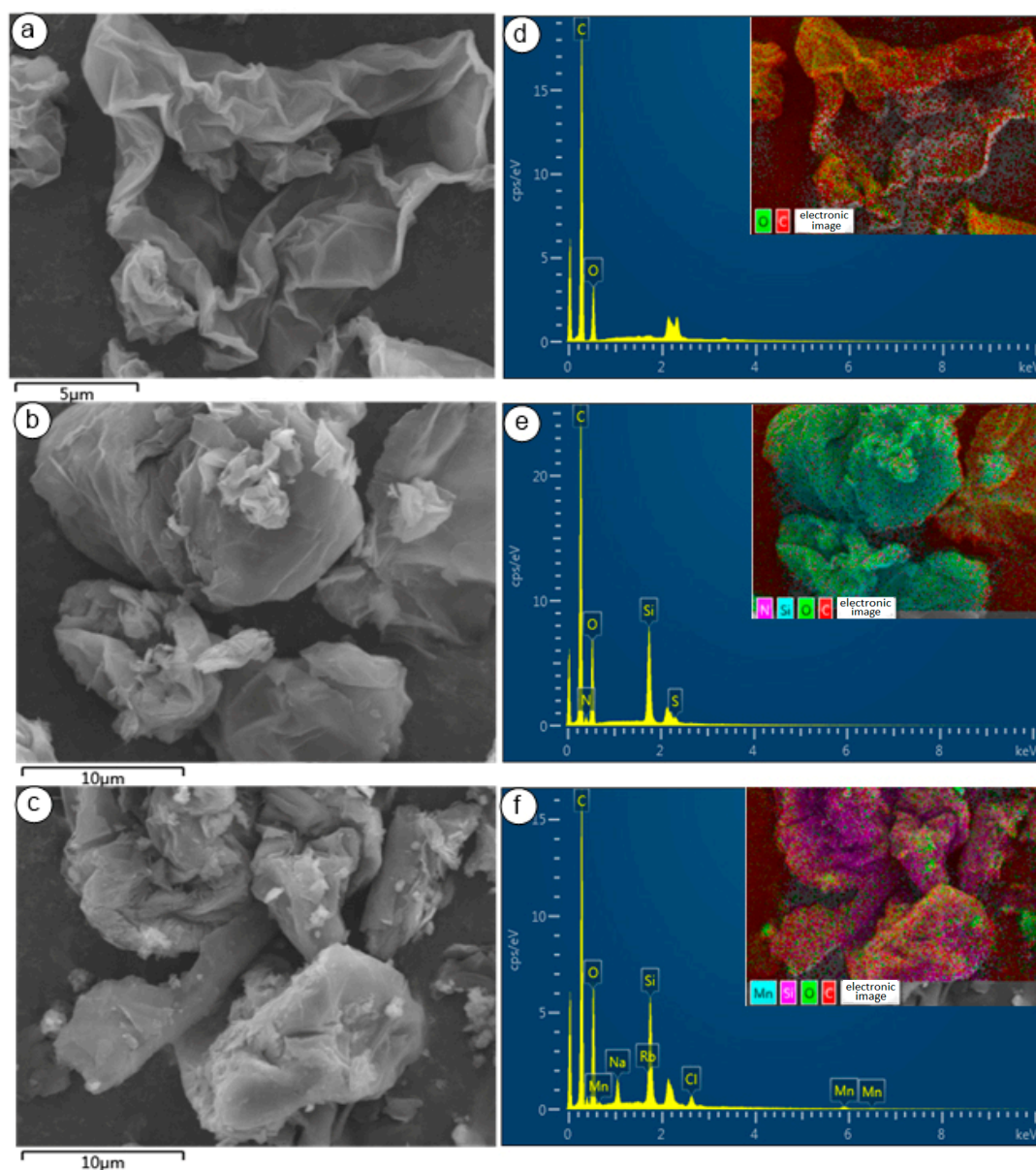


Figure 5. SEM photograph of (a) GO, (b) GO-NH₂, and (c) GO-salenMn, and the measured EDS image of (d) GO, (e) GO-NH₂, and (f) GO-salenMn.

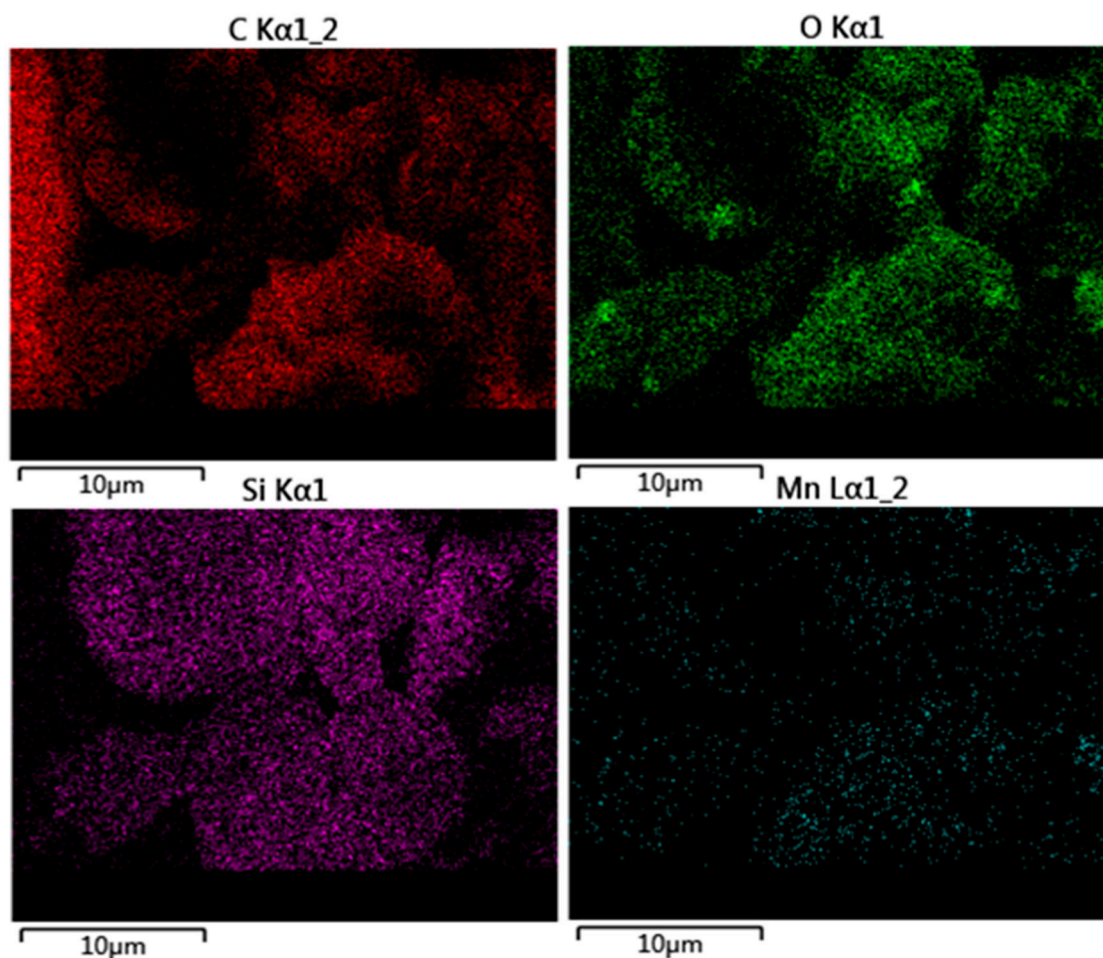


Figure 6. EDS elementary mapping of (a) C, (b) O, (c) Si, and (d) Mn in GO-salenMn.

2.5. XRD Analysis

The XRD results of GO, GO-NH₂, and GO-salenMn are shown in Figure 7. As seen in Figure 7a, a sharp diffraction peak at $2\theta = 10.76^\circ$ indicated the (001) characteristic diffraction of GO. A small diffraction peak appeared at 10° – 26° , which was caused by the superposition of the laminate crystallization of GO with different thicknesses. This further proved that GO had been successfully prepared. Figure 7b,c shows no characteristic diffraction peak of GO, indicating that the original layer-cumulative structure of GO had been changed in the process of amine functionalization. In addition, after the homogeneous salenMn catalyst reacted with GO-NH₂, possibly due to the insertion of homogeneous salenMn catalyst between residual layers, the structure of GO-NH₂ was further destroyed, and the aggregation degree decreased. Combined with SEM analysis, these data show that GO-NH₂ and GO-salenMn became amorphous.

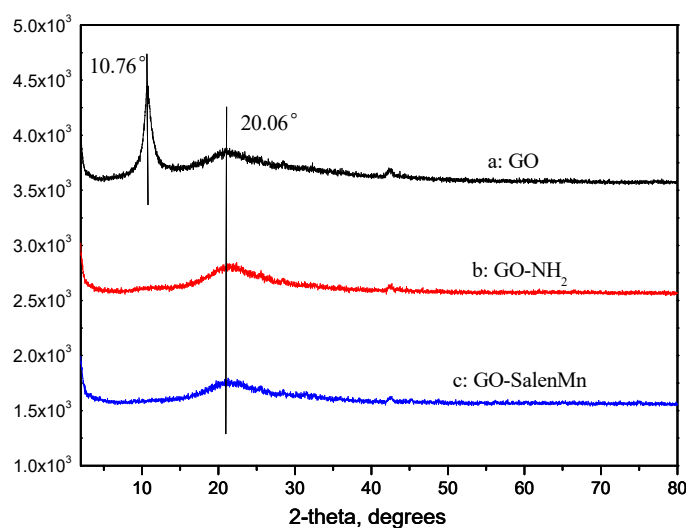


Figure 7. X-ray spectra of (a) GO, (b) GO-NH₂, and (c) GO-salenMn.

2.6. Asymmetric Epoxidation

Using *m*-CPBA/NMO as an oxidation system, the performance of salenMnCl and GO-salenMn catalysts for asymmetric epoxidation of α -methyl-styrene, styrene, and indene under the same conditions was compared. In addition, the performance of the catalytic reaction with or without the participation of axial additive NMO was studied in detail. The results are shown in Table 1. The results showed that the GO-salenMn catalyst could effectively catalyze epoxidation of alkenes (entries 2, 5, and 8). Compared with homogeneous salenMnCl, the GO-salenMn catalyst significantly increased the enantiomeric excess (*ee*) value of epoxides (entries 2, 5, and 8). The *ee* value of α -methyl-styrene epoxide increased from 52.0 to 83.2%. Similar results were observed in epoxidation of styrene and indene. The increase in chiral recognition was mainly attributed to the layered support effect [29]. In contrast, another GO-salenMn catalyst [26], where salenMnCl was immobilized on amino-modified GO or imidazolium-based ionic liquid-functionalized GO with the methyl chloride group ($-\text{CH}_2\text{Cl}$) at the fifth position of the chiral salen ligand, gave a slightly lower *ee* value in the NaClO/PyNO oxidation system. The results showed that the combined effect of the immobilization mode and the oxidation system was beneficial to increase the *ee* value. Moreover, in our previous reports, the ZPS-PVPA-based catalyst-effectively catalyzed epoxidation of styrene and α -methyl-styrene (*ee*: 50 to 78% and 86% to >99%) with *m*-CPBA or NaClO. These results are significantly better than those achieved with the homogeneous chiral catalysts under the same reaction conditions (*ee*: 47% and 65%). Moreover, the immobilized catalysts could be reused at least 10 times without significant loss of activity and enantioselectivity. Furthermore, a point worth emphasizing is that the ZPS-PVPA-based catalyst resulted in remarkable increase of conversion and *ee* values in the absence of expensive NMO for the asymmetric epoxidation of olefins, which is exactly opposite to the literature reported earlier for both homogeneous and heterogeneous systems. This novel additive effect was mainly attributed to the support ZPS-PVPA and the axial phenoxy linker group [10], α -methyl-styrene. Regrettably in this study, the *ee* values were sharply decreased when the epoxidation was carried out with GO-salenMn in the absence of axial ligand NMO (entries 3, 6, and 9). The results demonstrated that the NMO could coordinate with oxo-salenMn (V) and stabilize the generated intermediate oxo-salenMn (V) complex [30], so that the substrates and catalysts could fully react.

Table 1. Asymmetric epoxidation of different substrates by salenMnCl and GO-salenMn ^a.

Entry	Substrate	Catalyst	Oxidant	Time (h)	Conv (%) ^b	Sele (%) ^b	ee (%) ^b	TOF ^e × 10 ⁻⁴ (s ⁻¹)
1		salenMnCl	<i>m</i> -CPBA/NMO	1	>99	>99	52.0 ^c	27.2
2		GO-salenMn	<i>m</i> -CPBA/NMO	2	>99	>99	83.2 ^c	13.5
3		GO-salenMn	<i>m</i> -CPBA	2	65.9	76.5	8.6 ^c	7.0
4		salenMnCl	<i>m</i> -CPBA/NMO	1	>99	>99	46.2 ^c	27.1
5		GO-salenMn	<i>m</i> -CPBA/NMO	2	92.5	93.1	67.8 ^c	12.0
6		GO-salenMn	<i>m</i> -CPBA	2	73.2	72.9	5.9 ^c	7.4
7		salenMnCl	<i>m</i> -CPBA/NMO	1	>99	>99	65.0 ^d	27.2
8		GO-salenMn	<i>m</i> -CPBA/NMO	2	>99	>99	83.2 ^d	13.6
9		GO-salenMn	<i>m</i> -CPBA	2	77.9	81.6	13.1 ^d	8.8

^a Reactions were carried out in CH₂Cl₂ (3 mL) with alkene (0.5 mmol), *m*-CPBA (1.0 mmol), NMO (2.5 mmol, if necessary), nonane (internal standard, 0.5 mmol), and GO-salenMn (0.010 mmol, 2.0 mol%), based on elemental Mn at 0 °C. ^b Conversions, selectivity, and enantiomeric excess (*ee*) values were determined by GC with a chiral capillary column (HP19091G-B233, 30 m × 0.25 mm × 0.25 μm) by integration of product peaks against an internal quantitative standard (nonane), correcting for response factors. ^c Epoxide configuration R. ^d Epoxide configuration 1R, 2S. ^e Turnover frequency (TOF) is calculated by the expression of [product]/[catalyst] × time (s⁻¹).

2.7. Investigation of Reuse Performance of Supported Catalysts

The reuse performance of solid catalysts is an important standard to measure whether the catalytically active center has effectively and stably immobilized on the carrier. The reuse performance of GO-salenMn was studied in detail with α -methyl-styrene as the template reaction. The results are listed in Table 2 and show that the catalytic activity and enantioselectivity of the catalyst were not significantly changed after the catalyst was reused three times, and the conversion rate was still greater than 99%. With the increase in reuse times, enantioselectivity and chemical selectivity gradually decreased. However, even after the catalyst was reused 10 times, the *ee* value was still higher than 52%. However, compared with fresh catalysts, the yield dropped from 96.9 to 55.6%. A possible reason for deactivation of the GO-salenMn is the decomposition of salenMnCl under NaOH aqueous solution [31].

Table 2. The recycling of GO-salenMn in the epoxidation of α -methyl-styrene ^a.

Run	Conv (%) ^b	Sele (%) ^b	ee (%) ^{b,c}	TOF ^d × 10 ⁻⁴ (s ⁻¹)
1	>99	97.9	83.2	13.5
2	>99	97.0	83.0	13.3
3	>99	96.3	82.4	13.3
4	98.2	95.2	82.2	13.0
5	96.9	94.3	81.7	12.7
6	95.3	92.2	81.0	12.2
7	92.1	86.9	80.3	11.1
8	89.3	79.2	78.7	9.8
9	86.2	73.2	76.2	8.8
10	80.6	69.0	71.9	7.7

^{a,b,c} The reaction conditions are the same as those for Table 1. ^d Turnover frequency (TOF) is calculated by the expression of [product]/[catalyst] × time (s⁻¹).

3. Material and Methods

3.1. Materials

The chemicals (1R,2R)-(-)-1,2-diaminocyclohexane, α -methyl-styrene, indene, *n*-nonane, N-methylmorpholine N-oxide (NMO), *m*-chloroperbenzoic acid (*m*-CPBA), and γ -propyl mercaptotrimethoxysilane (MPTMS) were purchased from Alfa Aesar. The other commercially available chemicals that were procured were laboratory-grade reagents from local suppliers (Chuangdong Chemical Group Co., Ltd. Chongqing, China). Styrene was passed through a pad of neutral alumina before use. Chiral salen ligand and chiral salenMnCl complex were synthesized according to previously published procedures [1].

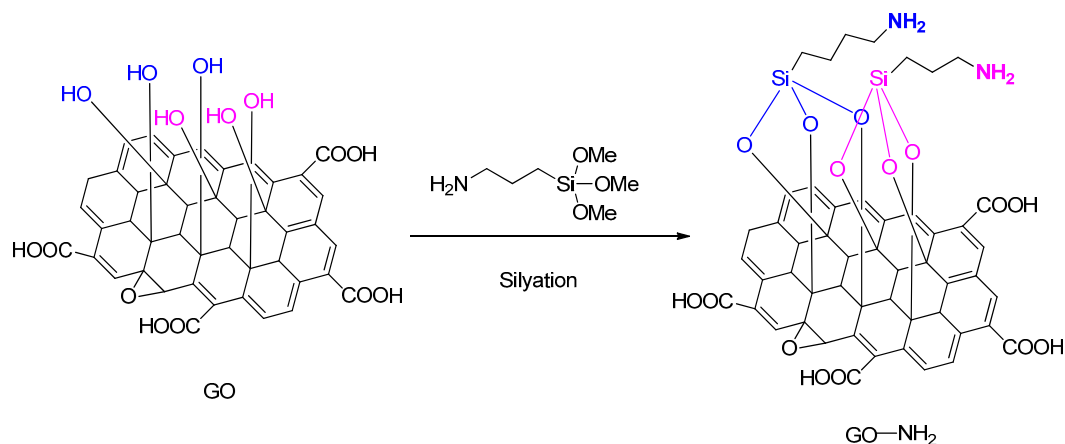
3.2. Methods

Fourier transform infrared (FT-IR) spectra were obtained as potassium bromide pellets with a resolution of 4 cm^{-1} in the range of $400\text{--}4000\text{ cm}^{-1}$ using a Bruker RFS100/S spectrophotometer (Bruker, Karlsruhe, Germany). Atomic absorption spectroscopy (AAS) was used to determine the Mn content of the catalysts using a TAS-986G (Pgeneral, Beijing, China), where 0.02 g of GO-salenMn was calcined at $700\text{ }^{\circ}\text{C}$ for 3 h, dissolved in 1:1 hydrochloric acid for 30 min, and the volume was adjusted. The loading of Mn^{2+} was measured by standard addition method. To explore the success of the GO-salenMn, high-resolution field emission scanning electron microscopy (FE-SEM, JSM 7800F, Tokyo, Japan) operating at 5 kV was used to analyze the topographic microstructure. Environmental SEM equipped with an energy dispersive (EDS) X-ray spectrometer was also used to investigate the composition and spatial distribution of elements in the samples. Scanning electron microscope (SEM) was carried out with a powder sample (100 mg) dispersed in alcohol (10 mL) and sonicated for 10 min. The dispersion was dripped onto the conductive tape, and the tape was blown dry with a blower and then tested. To carry out the EDS, the powder sample was put on a conductive adhesive cloth. The interlayer spacings were recorded on a LabXRD-6100 automated X-ray power diffractometer (XRD), using $\text{Cu K}\alpha$ radiation and internal silicon powder standard with all samples (Shimadzu, Kyoto, Japan). The patterns were generally measured between 2.00° and 80.00° and X-ray tube settings of 40 kV and 5 mA. Thermogravimetry–differential scanning calorimetry (TG–DSC) analyses (5 mg) were performed on a SBTQ600 thermal analyzer (TA, USA) with the heating rate of $10\text{ }^{\circ}\text{C}\cdot\text{min}^{-1}$ from 25 to $1000\text{ }^{\circ}\text{C}$ under flowing N_2 ($100\text{ mL}\cdot\text{min}^{-1}$). X-ray photoelectron spectroscopy (XPS) data were obtained with an ESCALab250 instrument (MA, USA) electron spectrometer using 75 W $\text{Al K}\alpha$ radiation. The base pressure was about 1×10^{-8} Pa. The conversions (with *n*-nonane as an internal standard) and the enantiomeric excess (*ee*) values were analyzed by gas chromatography (GC) with a Shimadzu GC-2014 instrument (Shimadzu, Japan) equipped with a chiral column (HP19091G-B233, $30\text{ m} \times 0.25\text{ mm} \times 0.25\text{ }\mu\text{m}$) and flame ionization detector; injector $230\text{ }^{\circ}\text{C}$, detector $230\text{ }^{\circ}\text{C}$. The column temperature for *a*-methylstyrene, styrene, and indene was $80\text{--}180\text{ }^{\circ}\text{C}$. The retention times of the corresponding chiral epoxides were as follows: (a) α -methyl-styrene epoxide: the column temperature was $80\text{ }^{\circ}\text{C}$, $t_{\text{S}} = 12.9\text{ min}$, $t_{\text{R}} = 13.0\text{ min}$; (b) styrene epoxide: the column temperature was $80\text{ }^{\circ}\text{C}$, $t_{\text{R}} = 14.7\text{ min}$, $t_{\text{S}} = 14.9\text{ min}$; (c) indene epoxide: the column temperature was programmed from 80 to $180\text{ }^{\circ}\text{C}$, $t_{\text{SR}} = 16.1\text{ min}$, $t_{\text{RS}} = 17.1\text{ min}$.

4. Preparation of Catalysts

4.1. Synthesis of GO and GO-NH₂

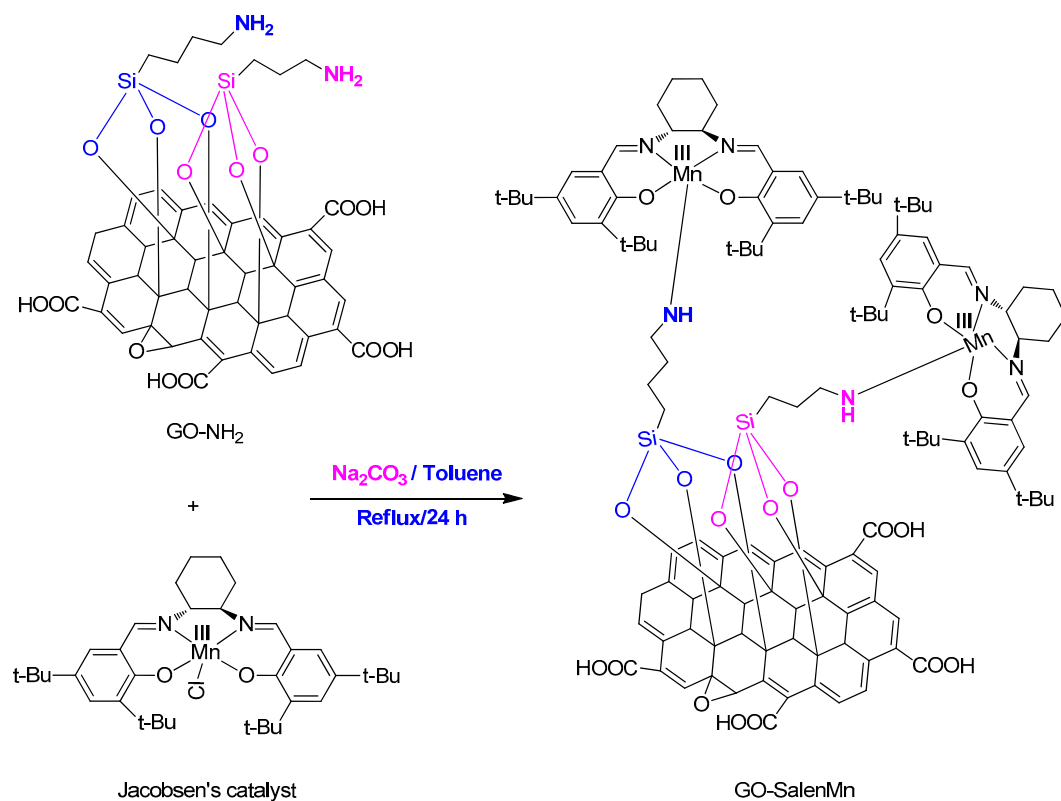
The parent GO was prepared by the previously reported Hummers method [32,33]. Then, 0.50 g of GO was dispersed in 20 mL of anhydrous toluene. After ultrasonication for 2.0 h, a certain amount of APTES was added and stirred for 12 h under reflux [34] (Scheme 1). The solid was collected by filtration, washed with dichloromethane, and vacuum-dried at $60\text{ }^{\circ}\text{C}$ for 10 h. The final catalyst was defined as amine-functionalized graphene oxide: GO-NH₂, yield: 93.6%.



Scheme 1. Synthesis of GO-NH₂.

4.2. Synthesis of GO-salenMn Catalyst

In a 50 mL three-neck flask, 0.2 g amination carrier GO-NH₂ was pre-added to 10 mL toluene for undergoing ultrasonication for 30 min, followed by homogeneous chiral salenMnCl catalyst (543 mg, 1.0 mmol), Na₂CO₃ (120 mg, 3 mmol), and 20 mL toluene; the solution underwent reflux reaction for 24 h (Scheme 2). After the reaction stopped, the mixture was cooled to room temperature. Then, the solid mixture was soaked in methylene chloride, filtered by extraction, and centrifugally washed in methylene chloride and ethanol successively until the filtrate was clarified. The final filtrate was collected and tested by AAS, which showed no presence of Mn²⁺. The brown solid catalyst powder was prepared by 60 °C vacuum drying to constant weight and the yield was 90.3%. AAS showed that the loading of the supported catalyst Mn²⁺ was 0.39 mmol/g.



Scheme 2. Synthesis of the immobilized catalysts.

4.3. Asymmetric Epoxidation

At 0 °C, substrate (0.5 mmol), NMO (337.5 mg, 2.5 mmol, 5 equiv., if necessary), nonane (internal standard, 56.0 mL, 0.50 mmol), and a certain amount of GO-salenMn (0.010 mmol, 2.0%, manganese-based) were successively added to 3 mL CH₂Cl₂ solution. The oxidant *m*-CPBA (138 mg, 1.0 mmol, 2 equiv.) was added to the thermostatic reaction system in four portions within two minutes. After the reaction, NaOH aqueous solution (1 mol/L, 1.25 mL) was added to the system until the pH value was slightly higher than 7. After *n*-hexane was added, organic phase was extracted and dried by anhydrous sodium sulfate. Then column chromatography was conducted, and the chromatography liquid was rotated–evaporated and directly injected into the gas chromatograph to analyze the conversion rate and enantioselectivity. The racemic epoxides were prepared by epoxidation of the corresponding olefins by *m*-CPBA in CH₂Cl₂ and confirmed by NMR, and the GC was calibrated with the samples of *n*-nonane, olefins, and corresponding racemic epoxides.

4.4. Repeated Experiments of Supported Mn(Salen) Catalyst

In order to investigate the reuse performance of supported catalysts, α -methyl-styrene was used as a substrate. After the initial reaction, *n*-hexane was added directly to the reaction system and oscillated, and the organic phase at the top was separated after standing, and the supported catalyst at the bottom was removed and successively washed by distilled water, dichloromethane, and ethanol, and then dried for future use. Subsequent cycling with different amounts and product analysis was performed according to Section 4.3.

5. Conclusions

In summary, a simple and effective heterogeneous catalyst, GO-salenMn, was developed in this study and characterized in detail by FT–IR, TG–DSC, XPS, EDS, SEM, XRD, and AAS. The successful preparation of GO-salenMn was confirmed. GO-salenMn can efficiently catalyze α -methyl-styrene, styrene, and indene in *m*-CPBA/NMO as the oxidation system, and in particular, epoxides can be obtained with higher enantioselectivity than those obtained by homogeneous salenMnCl catalyst. However, enantioselectivity significantly decreased without the participation of axial promoter NMO. After the supported catalyst was reused 10 times, the *ee* value of α -methyl-styrene epoxides was still higher than that obtained by the homogeneous salenMnCl catalyst under the same conditions. However, after the catalyst was reused six times, the selectivity of the catalyst significantly decreased. The cause of catalyst deactivation still requires further investigation.

Author Contributions: X.Z. designed the experiments, wrote the paper, and provided the funds; F.W., T.H., S.R., Q.C., and X.D. performed the experiments; Z.T. and C.H. provided analytical testing.

Funding: This work was financially supported by the Children’s Research Institute of National Center for the Schooling Development Programme and Chongqing University of Education (grant no. CSDP19FS01111), the Natural Science Foundation of Chongqing (no. cstc2018jcyjAX0110), the Science and Technology Research Program of Chongqing Municipal Education Commission (no. KJ201801607), the Key Laboratory for Green Chemical Technology of Chongqing University of Education (no. 2016xjpt08), and the “Qizhi” Creative Space Student Entrepreneurship Incubation Project of Chongqing University of Education (2019).

Conflicts of Interest: The authors declare no conflict of interest.

References

1. Zhang, W.; Loebach, J.L.; Wilson, S.R.; Jacobsen, E.N. Enantioselective epoxidation of unfunctionalized olefins catalyzed by salen manganese complexes. *J. Am. Chem. Soc.* **1990**, *112*, 2801–2803. [[CrossRef](#)]
2. Luo, Y.F.; Zou, X.C.; Fu, X.K.; Jia, Z.Y.; Huang, X.M. The advance in asymmetric epoxidation of olefins catalyzed by chiral Mn(salen). *Sci. China Chem.* **2011**, *41*, 433–450.
3. Zhang, H.D.; Zhang, Y.M.; Li, C. Asymmetric epoxidation of unfunctionalized olefins catalyzed by Mn(salen) axially immobilized onto insoluble polymers. *Tetrahedron Asymmetry* **2005**, *16*, 2417–2423. [[CrossRef](#)]

4. Aneta, N.; Agnieszka, W.; Michael, W. Recent advances in the catalytic oxidation of alkene and alkane substrates using immobilized manganese complexes with nitrogen containing ligands. *Coord. Chem. Rev.* **2019**, *382*, 181–216.
5. Reger, T.S.; Janda, K.D. Polymer-Supported (Salen)Mn Catalysts for Asymmetric Epoxidation: A Comparison Between Soluble and Insoluble Matrices. *J. Am. Chem. Soc.* **2000**, *122*, 6929–6934. [[CrossRef](#)]
6. Peng, M.; Chen, Y.J.; Tan, R.; Zheng, W.G.; Yin, D.H. A highly efficient and recyclable catalyst-dendrimer supported chiral salen Mn(III) complexes for asymmetric epoxidation. *RSC Adv.* **2013**, *3*, 20684–20692. [[CrossRef](#)]
7. Afsaneh, F.; Hassan, H.M. Highly efficient asymmetric epoxidation of olefins with a chiral manganese-porphyrin covalently bound to mesoporous SBA-15: Support effect. *J. Catal.* **2017**, *352*, 229–238.
8. Zou, X.C.; Shi, K.Y.; Li, J.; Wang, Y.; Deng, C.F.; Wang, C.; Ren, Y.R.; Tan, J. Research Progress on Epoxidation of Olefins Catalyzed by Mn(II, III, V) in Different Valence States. *Chin. J. Org. Chem.* **2016**, *36*, 1765–1778. [[CrossRef](#)]
9. Gong, B.W.; Fu, X.K.; Chen, J.X.; Li, Y.D.; Zou, X.C.; Tu, X.B.; Ding, P.P.; Ma, L.P. Synthesis of a new type of immobilized chiral salen Mn(III) complex as effective catalysts for asymmetric epoxidation of unfunctionalized olefins. *J. Catal.* **2009**, *262*, 9–17. [[CrossRef](#)]
10. Zou, X.C.; Fu, X.K.; Li, Y.D.; Tu, X.B.; Fu, S.D.; Luo, Y.F.; Wu, X.J. Highly enantioselective epoxidation of unfunctionalized olefins catalyzed by chiral Jacobsen's catalyst immobilized on phenoxyl modified Zirconium poly (styrene-phenylvinylphosphonate)-phosphate. *Adv. Synth. Catal.* **2010**, *352*, 163–170. [[CrossRef](#)]
11. Zou, X.C.; Wang, C.; Wang, Y.; Shi, K.Y.; Wang, Z.M.; Li, D.W.; Fu, X.K. Chiral Mn(III) (Salen) Covalently Bonded on Modified ZPS-PVPA and ZPS-IPPA as Efficient Catalysts for Enantioselective Epoxidation of Unfunctionalized Olefins. *Polymers* **2017**, *9*, 108. [[CrossRef](#)]
12. Zou, X.C.; Shi, K.Y.; Wang, C. Chiral Mn(III)(Salen) supported on tunable phenoxyl group modified zirconium poly (styrene-phenylvinylphosphonate)-phosphate as an efficient catalyst for epoxidation of unfunctionalized olefins. *Chin. J. Catal.* **2014**, *35*, 1446. [[CrossRef](#)]
13. Huang, J.; Liu, S.R.; Ma, Y.; Cai, J.L. Chiral salen Mn (III) immobilized on ZnPS-PVPA through alkoxy-triazole for superior performance catalyst in asymmetric epoxidation of unfunctionalized olefins. *J. Organomet. Chem.* **2019**, *886*, 27–33. [[CrossRef](#)]
14. Huang, X.M.; Fu, X.K.; Jia, Z.Y.; Miao, Q.; Wang, G.M. Chiral salen Mn(III) complexes immobilized onto crystalline aluminium oligo-styrenyl phosphonate-hydrogen phosphate (AlSPP) for heterogeneous asymmetric epoxidation. *Catal. Sci. Technol.* **2013**, *3*, 415–424. [[CrossRef](#)]
15. Huang, J.; Tang, M.; Li, X.; Zhong, G.Z.; Li, C.M. Novel layered crystalline organic polymer-inorganic hybrid material comprising calcium phosphate with unique architectures for superior performance catalyst support. *Dalton Trans.* **2014**, *43*, 17500–17508. [[CrossRef](#)] [[PubMed](#)]
16. Li, Z.F.; Yang, C.L.; Cui, J.X.; Ma, Y.Y.; Kan, Q.B.; Guan, J.Q. Recent Advancements in Graphene-Based Supports of Metal Complexes/Oxides for Epoxidation of Alkenes. *Chem. Asian J.* **2018**, *13*, 3790–3799. [[CrossRef](#)]
17. Siegfried, E.; Andreas, H. Chemistry with graphene and graphene oxide-challenges for synthetic chemists. *Angew. Chem. Int. Ed.* **2014**, *53*, 7720–7738.
18. Scheuermann, G.M.; Rumi, L.; Steurer, P.; Bannwarth, W.; Mühlaupt, R. Palladium nanoparticles on graphite oxide and its functionalized graphene derivatives as highly active catalysts for the Suzuki-Miyaura coupling reaction. *J. Am. Chem. Soc.* **2009**, *131*, 8262–8270. [[CrossRef](#)]
19. Shao, L.D.; Huang, X.; Teschner, D.; Zhang, W. Gold Supported on Graphene Oxide: An Active and Selective Catalyst for Phenylacetylene Hydrogenations at Low Temperatures. *ACS Catal.* **2014**, *4*, 2369–2373. [[CrossRef](#)]
20. Li, X.; Yu, J.G.; Wageh, S.; Ghamdi, A.A.A.; Xie, J. Graphene in Photocatalysis: A Review. *Small* **2016**, *12*, 6640–6696. [[CrossRef](#)]
21. Liang, Y.Y.; Wang, H.L.; Casalongue, H.S.; Chen, Z.; Dai, H.J. TiO₂ nanocrystals grown on graphene as advanced photocatalytic hybrid materials. *Nano Res.* **2010**, *3*, 701–705. [[CrossRef](#)]
22. Yun, M.; Ahmed, M.S.; Jeon, S. Thiolated graphene oxide-supported palladium cobalt alloyed nanoparticles as high performance electrocatalyst for oxygen reduction reaction. *J. Power Sources* **2015**, *293*, 380–387. [[CrossRef](#)]

23. Yuan, D.C.; Chen, B.B. Synthesis and Characterization of Graphene Oxide Supported Schiff Base Palladium Catalyst and Its Catalytic Performance to Suzuki Reaction. *Chin. J. Org. Chem.* **2014**, *34*, 1630–1638. [[CrossRef](#)]
24. Tan, R.; Li, C.Y.; Luo, J.Q.; Kong, Y.; Zheng, W.G.; Yin, D.H. An effective heterogeneous L-proline catalyst for the direct asymmetric aldol reaction using graphene oxide as support. *J. Catal.* **2013**, *298*, 138–147. [[CrossRef](#)]
25. Shi, H.; Yu, C.; He, J. On the Structure of Layered Double Hydroxides Intercalated with Titanium Tartrate Complex for Catalytic Asymmetric Sulfoxidation. *J. Phys. Chem. C* **2010**, *114*, 17819–17828. [[CrossRef](#)]
26. Zheng, W.G.; Tan, R.; Yin, S.F.; Zhang, Y.Y.; Zhao, G.W.; Chen, Y.J.; Yin, D.H. Ionic liquid-functionalized graphene oxide as an efficient support for the chiral salen MnIII complex in asymmetric epoxidation of unfunctionalized olefins. *Catal. Sci. Technol.* **2015**, *5*, 2092–2102. [[CrossRef](#)]
27. Domenech, A.; Formentin, P.; Garcia, H.; Sabater, M.J. Combined electrochemical and EPR studies of manganese Schiff base complexes encapsulated within the cavities of zeolite Y. *Eur. J. Inorg. Chem.* **2000**, *2000*, 1339–1344. [[CrossRef](#)]
28. Zou, X.C.; Wang, Y.; Wang, C.; Shi, K.Y.; Ren, Y.R.; Zhao, X. Chiral MnIII (Salen) Immobilized on Organic Polymer/Inorganic Zirconium Hydrogen Phosphate Functionalized with 3-Aminopropyltrimethoxysilane as an Efficient and Recyclable Catalyst for Enantioselective Epoxidation of Styrene. *Polymers* **2019**, *11*, 212. [[CrossRef](#)]
29. Caplan, N.A.; Hancock, F.E.; Bulman, P.P.C.; Hutchings, G.J. Heterogeneous Enantioselective Catalyzed Carbonyl- and Imino-Ene Reactions using Copper Bis(Oxazoline) Zeolite, Y. *Angew. Chem. Int. Ed.* **2004**, *43*, 1685–1688. [[CrossRef](#)]
30. Venkataramanana, N.S.; Rajagopal, S. Effect of added donor ligands on the selective oxygenation of organic sulfides by oxo(salen)chromium(V) complexes. *Tetrahedron* **2006**, *62*, 5645–5651. [[CrossRef](#)]
31. Ma, X.B.; Wang, Y.H.; Wang, W.; Cao, J. Synthesis and characterization of mesoporous zirconium phosphonates: A novel supported cinchona alkaloid catalysts in asymmetric catalysis. *Catal. Commun.* **2010**, *11*, 401–407. [[CrossRef](#)]
32. Jia, H.P.; Dreyer, D.R.; Bielawski, C.W. Graphite Oxide as an Auto-Tandem Oxidation–Hydration–Aldol Coupling Catalyst. *Adv. Synth. Catal.* **2011**, *53*, 528–532. [[CrossRef](#)]
33. Zou, Z.G.; Yu, H.J.; Long, F.; Fan, Y.H. Preparation of Graphene Oxide by Ultrasound-Assisted Hummers Method. *Chin. J. Inorg. Chem.* **2011**, *27*, 1753–1757.
34. Zhang, F.; Jiang, H.Y.; Li, X.Y.; Wu, X.T.; Li, H.X. Amine-Functionalized GO as an Active and Reusable Acid–Base Bifunctional Catalyst for One-Pot Cascade Reactions. *ACS Catal.* **2014**, *4*, 394–401. [[CrossRef](#)]



© 2019 by the authors. Licensee MDPI, Basel, Switzerland. This article is an open access article distributed under the terms and conditions of the Creative Commons Attribution (CC BY) license (<http://creativecommons.org/licenses/by/4.0/>).